Available online at www.sciencedirect.com
SCIENCE DIRECT®
Journal of Photochemistry and Photobiology A: Chemistry 164 (2004) 111–115
Journal of Photochemistry and Photobiology A:Chemistry
www.elsevier.com/locate/jphotochem

Electrochemical properties of dye-sensitized solar cells fabricated with PVDF-type polymeric solid electrolytes

Tsuyoshi Asano, Takaya Kubo, Yoshinori Nishikitani*

Central Technical Research Laboratory, Nippon Oil Corporation, 8 Chidori-cho, Naka-ku, Yokohama 231-0815, Japan

Received 25 July 2003; received in revised form 15 December 2003; accepted 26 December 2003

Abstract

We have already proposed a poly(vinylidenefluoride-co-hexafluoropropylene) (PVDF-HFP)-based polymeric solid electrolyte (PSE) film for dye-sensitized solar cells (DSSCs). The employment of the PSE film, however, almost always accompanies with decrease in short-circuit current density (J_{sc}). We then studied electrochemical properties on the PSE-based and liquid electrolyte-based DSSCs to clarify the reason why the conversion efficiency is lower in the former than in the latter. The diffusion coefficient of I_3^- and the cell gap of DSSCs were found out to play a key role to increase J_{sc}. In particular, the stronger cell-gap dependence was observed in the PSE-based DSSC than in the liquid electrolyte-based DSSC. This indicates that the design of DSSC structure is quite important to achieve the higher conversion efficiency in the PSE-based DSSC. We confirmed that the J_{sc} of a PSE-based DSSC with a 20 μm cell gap is turned out to be about 97% of the J_{sc} of a liquid electrolyte-based DSSC.

Keywords: PVDF; DSSC; Electrolyte; Polymeric solid electrolyte

1. Introduction

Dye-sensitized solar cells (DSSCs) were first studied extensively by Tsubomura et al. in 1976 [1]. The conversion efficiency of the solar cells was then about 1%. O'Regan and Grätzel made a major breakthrough in the conversion efficiency in 1991 [2] and opened up the possibilities of practical applications as solar cells. A DSSC comprises an electrode consisting of a nanocrystalline TiO_2 layer with ruthenium sensitizer adsorbed on the TiO_2 surface, a counter electrode consisting of a F-doped SnO_2 substrate with a Pt thin layer coated on top of it, and an electrolyte solution with a I^-/I_3^- redox couple.

DSSCs are attractive for next-generation solar cells not only because of their potentially high conversion efficiency but also because of the lower production cost of DSSCs than that of conventional silicon solar cells [3]. However, many things, such as increasing the conversion efficiency even more and achieving better durability, remain to be done before DSSCs can be put on the market [4–8]. The electrolyte loss caused by the leakage and/or volatility of the electrolyte solution has been pointed out to be one of the major problems, which stays the durability of the DSSC low. Various approaches to the problem have been tried so far. These approaches include employing a gel-type electrolyte to minimize the loss [9–13], or replacing the liquid electrolyte with either p-type solid inorganic semiconductors or conducting organic materials to avoid the loss completely [14–22]. The gel-type electrolyte appears to give rise to successful results in terms of a conversion efficiency among these approaches. Wang et al. recently employed a polymeric gel electrolyte containing 1-methyl-3-propylimidazolium iodide and poly(vinylidenefluoride-co-hexafluoropropylene) (PVDF-HFP) to fabricate a DSSC, and the conversion efficiency of that DSSC with a 0.152 cm^2 active area at AM 1.5 illumination stayed at 5.3% [23]. We proposed a PVDF-HFP-based polymeric solid electrolyte (PSE) film for DSSCs [24,25]. The film allows us to obtain a short-circuit current density (J_{sc}) higher than 70% of that of a DSSC with a liquid electrolyte. Although these measures are effective in reducing or avoiding electrolyte loss, they almost always cause the conversion efficiency to decrease.

The purpose of this paper is two-fold: (1) we elucidate the reason why the conversion efficiency is lower in PSE-based DSSCs than in liquid electrolyte-based DSSCs, and (2) obtain a guiding principle for the design of the PSE-based DSSC with a high enough conversion efficiency and equal to that of the liquid electrolyte-based DSSC.

* Corresponding author. Tel.: +81-45-625-7179; fax: +81-45-625-7298.
E-mail address: yoshinori.nishikitani@eneos.co.jp (Y. Nishikitani).

1010-6030/$ – see front matter © 2004 Elsevier B.V. All rights reserved.
doi:10.1016/j.jphotochem.2003.12.021

2. Experimental

All reagents were commercially available and used as-purchased. TiO_2 paste (Ti-nanoxide-T, Solaronix) was coated on a F-doped SnO_2 (FTO) substrate (TEC15, about 15 Ω/sq, Pilkington) using a Baker-applicator. The thickness of an as-coated TiO_2 film is about 250 μm and was then pre-cured at about 90 °C followed by heat treatment at 450 °C for 1 h. The TiO_2 films formed on the FTO were 10 μm thick and 5 mm × 5 mm in size. The TiO_2 substrate was immersed in ruthenium sensitizer (referred to hereafter as "dye") solution (0.5 mmol/l ruthenium-535-bis-TBA, Solaronix, in EtOH) for 20 h to let the nanosized-TiO_2 layer adsorb the dye, and the excess amount of dye was then rinsed off with EtOH. A 30 nm thick Pt thin film was deposited on the FTO substrate with the ion plating method, and was used as a counter electrode.

The electrolyte solution used in the liquid electrolyte-based DSSC is composed of 0.5 mol/l 1-propyl-2,3-dimethylimidazolium iodide (DMPII), 0.1 mol/l LiI, 0.05 mol/l I_2, 0.5 mol/l 4-*tert*-butylpyridine (TBP), and one of the following solvents to change the viscosity of the electrolyte solution and thus to change the diffusion coefficient of I_3^-: methoxyacetonitrile (MAN), 3-methoxypropionitrile (MPN), γ-butyrolactone (GBL), and propylene carbonate (PC). The viscosity of the solvent was measured at 25 °C with a viscosity meter (Viscomate VM-1G, Yamaichi electronics Co. Ltd.). The PSE film consists in the PVDF-HFP-based matrix polymer and an electrolyte solution (0.5 mol/l 1-propyl-2,3-dimethylimidazolium iodide, 0.1 mol/l LiI, 0.05 mol/l I_2, and 0.5 mol/l 4-*tert*-butylpyridine in γ-butyrolactone). The electrolyte solution and the matrix polymer were mixed with various contents depending on the purpose, and acetone was added to the mixture. The mixture was stirred at 70 °C until the polymer was dissolved completely. The mixture was then coated on a substrate with a doctor blade and left for 20 min at room temperature to dry. ^{1}H NMR analysis (JEOL EX-400) was carried out on a PSE film dissolved in dimethyl-d_6 sulfoxide, which confirmed no acetone residue in the film. The melting point was determined with a differential scanning calorimeter (Perkin Elmer DSC7). The polymer content of the PSE film was determined from the weight ratio of an as-formed PSE film to a dried, electrolyte-solution-free film. The diffusion coefficients (D_s) of I_3^- in the PSE films were evaluated using the Cottrell equation, $i(t) = nFAD^{1/2}C_0/\pi^{1/2}t^{1/2}$, where $n = 2$, F is the Faraday constant, C_0 the initial concentration of I_3^-, with the current decay curve obtained after applying a 0.6 V potential to a FTO/Pt/electrolyte/Pt/FTO cell [26].

The PSE-based DSSC was assembled by sandwiching a PSE film between the TiO_2-dye electrode and a Pt counter electrode and then sealing the perimeter of the cell while pressurizing it. The cell gap of the PSE-based DSSC was selected by changing the thickness of the PSE film to be prepared. The liquid electrolyte-based DSSC was assembled as follows: the two electrodes were held together with two pieces of a PET (polyethylene terephthalate) strips placed between the edges of the two electrodes; an electrolyte solution was introduced between the electrodes by capillary forces; the cell was then sealed along its perimeter. The cell gaps thus selected by tuning the thickness of the PET strips were measured with a micrometer (MDQ-30 Mitsutoyo Corporation). The cell gaps used are the length between the surfaces of the two FTO substrates.

The *I–V* characteristics were measured with a potentiostat (Schlumberger 1287 Solartron) under illumination (AM 1.5, 100 mW/cm^2, surface temperature of the DSSC at 27 °C) using a solar simulator (YSS-150, Yamashita-Denso Co. Ltd.) equipped with a cooling stage. *I–V* curves were obtained by scanning an applied potential to the DSSC between 1.5 and −0.5 V at a scan rate of 10 mV/s. Electrical impedance spectra were obtained in the frequency region from 10^{-2} to 10^6 Hz under illumination by applying sinusoidal perturbations of ±5 mV superimposed on the open-circuit voltage (V_{oc}). The electrical impedance spectra were analyzed using Z-View software (Solartron).

3. Results and discussion

3.1. Influence of the diffusion coefficient of I_3^- on the J_{sc} of DSSCs

The J_{sc} and V_{oc} values and diffusion coefficients of I_3^- of the liquid electrolyte-based and PSE-based DSSCs, and viscosities of the liquid electrolyte are tabulated in Table 1. The diffusion coefficients of the liquid electrolytes depend on their respective solvent (MAN, MPN, PC and GBL) viscosities, while those of the PSE film depend on the polymer contents (GBL/matrix polymer = 20.7, 27.5 and 37.0 mass%). In Fig. 1, the J_{sc} values given in Table 1 are plotted with the diffusion coefficient of I_3^-. The J_{sc}'s sharply increase with the diffusion coefficient and level off for larger values of the diffusion coefficient. The decrease in the diffusion coefficient reduces the supply of I_3^- to the Pt counter electrode, causing the depletion of I_3^- at the electrode and therefore

Table 1
The J_{sc} and V_{oc} values and diffusion coefficients of I_3^- of the liquid electrolyte-based and PSE-based DSSCs, and viscosities of the liquid electrolyte

Liquid electrolyte	D ($\times 10^6$ cm^2/s)	J_{sc} (mA/cm^2)	V_{oc} (V)	Viscosity (mPa s)
MAN	7.56	13.79	0.74	1.70
MPN	5.39	12.70	0.73	2.47
GBL	3.94	11.60	0.75	3.29
PC	2.72	10.02	0.70	4.64
PSE (GBL/matrix polymer) polymer content (mass%)				
20.7	2.26	10.75	0.75	–
27.5	1.90	10.10	0.70	–
37.0	1.06	6.28	0.75	–

MAN: methoxyacetonitrile, MPN: 3-methoxypropionitrile, GBL: γ-butyrolactone, and PC: propylene carbonate.

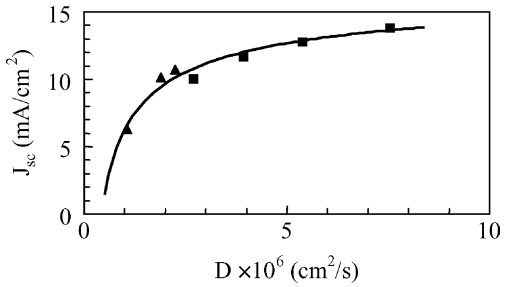

Fig. 1. Short-circuit current density (J_{sc}) of liquid electrolyte-based and PSE-based DSSCs with different diffusion coefficients of I_3^-: (■) liquid electrolyte-based DSSC; (▲) PSE-based DSSC.

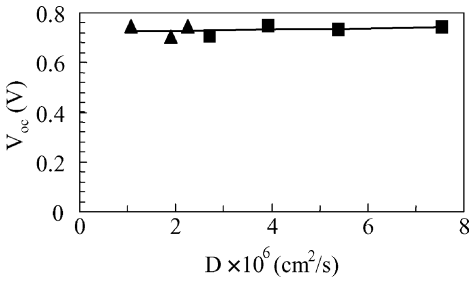

Fig. 2. Open-circuit voltage (V_{oc}) of liquid electrolyte-based and PSE-based DSSCs with different diffusion coefficients of I_3^-: (■) liquid electrolyte-based DSSC; (▲) PSE-based DSSC.

decreasing the J_{sc}. The ionic conductivity of the electrolyte, $\sigma = ne\mu$, is related to the diffusion coefficient of the supporting electrolyte through Einstein's relation, $D = \mu kT$: in the two equations, n is the carrier density, μ the mobility, k Boltzmann constant and T the temperature [27]. The decrease in the J_{sc} might originate from the decrease in the ionic conductivity. On the other hand, the J_{sc} tends to level off with increasing diffusion coefficient is caused mainly by the limited numbers of electrons available from the dye which is in turn limited by the absorption spectrum of the dye, i.e., photon limiting case.

As in Fig. 2, the diffusion coefficient dependence of the V_{oc} that we observed is quite weak and its variation is within 4%. The reverse-electron transfer from TiO_2 to I_3^- is reported to reduce V_{oc} because the electron density in the conduction band of TiO_2 decreases [28]. In an open-circuit condition, the concentration of I_3^- is expected to be constant over the entire distance between the TiO_2 and Pt counter electrodes irrespective of the diffusion coefficient of I_3^-. Hence, the V_{oc} is independent of the diffusion coefficient of I_3^-.

There is a possibility that the reverse-electron transfer is responsible for decreasing the J_{sc}. However, a close study still needs to be carried out on the electro- and photochemistry at the TiO_2/dye/electrolyte interface, combined with relevant model equations for the reactions inside the DSSC, to interpret the role of the reverse-electron transfer reaction in determining the J_{sc}.

Fig. 3 shows the electrical impedance spectra of the PSE-based DSSCs with five different polymer contents. All of the electrical impedance spectra exhibit three semicircles (A, B, and C), which are assigned, respectively, to the electrochemical reaction at the Pt counter electrode, the reaction at the TiO_2/dye electrode, and the diffusion process of I_3^- at the Pt/electrolyte interface [24,29]. We employed the equivalent circuit given in Fig. 4 for the curve fitting of the impedance spectra of DSSCs. The parameters obtained by fitting the impedance spectra with this equivalent circuit are summarized in Table 2. The symbol R_i (i = 1, 2) indicates the charge transfer resistance of the electrochemical reaction; R_s is the series resistance composed of the resistance of the electrolyte, TiO_2, the sheet resistance of the FTO film, and so

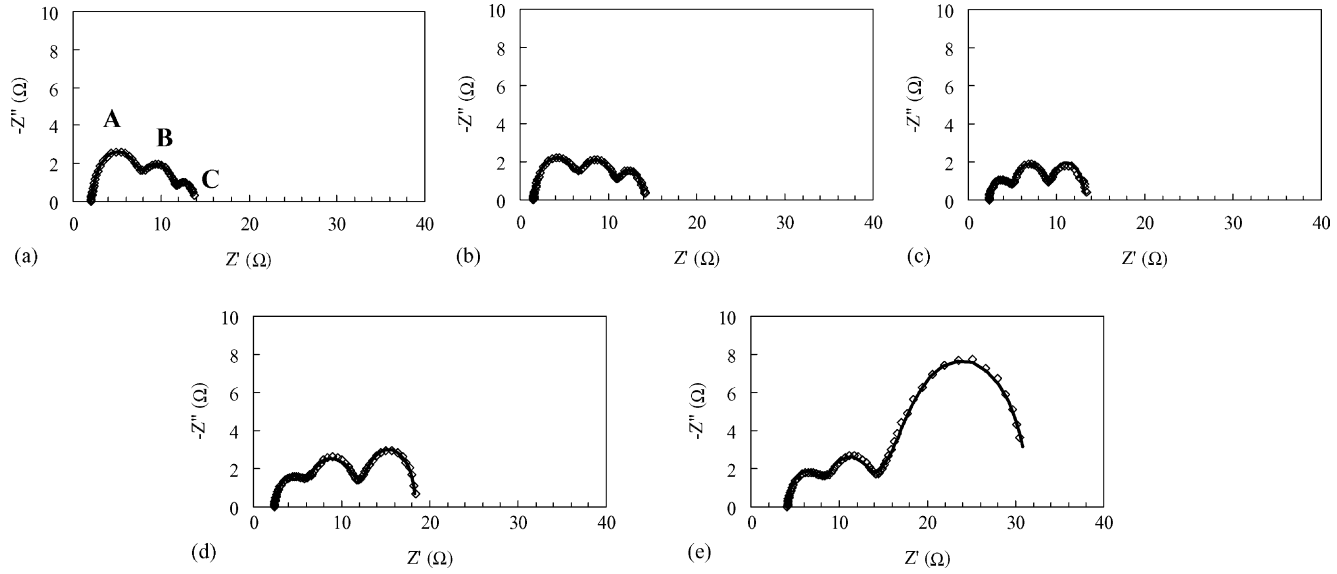

Fig. 3. Electrical impedance spectra of DSSCs with five different polymer contents: (a) 0 mass%; (b) 22.1 mass%; (c) 26.3 mass%; (d) 32.8 mass%; (e) 48.1 mass%.

Table 2
Numerical values for each element in the equivalent circuit obtained on DSSCs with five different polymer contents

Polymer content (mass%)	R_s (Ω)	R_1 (Ω)	R_D (Ω)	τ (s)	T_1 (mF)	P_1	R_2 (Ω)	T_2 (mF)	P_2
0	2.05	5.69	2.42	0.86	0.061	0.91	3.66	2.57	0.92
22.1	1.50	4.86	3.49	1.08	0.074	0.90	4.12	2.97	0.89
26.3	1.92	3.54	4.43	1.82	0.051	0.94	3.80	3.12	0.90
32.8	2.37	3.53	7.10	3.62	0.147	0.87	5.36	3.15	0.87
48.1	4.15	4.04	18.31	8.58	0.085	0.89	5.04	2.54	0.88

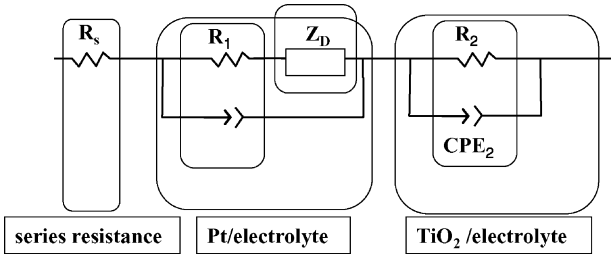

Fig. 4. Equivalent circuit model of the impedance spectra of DSSCs.

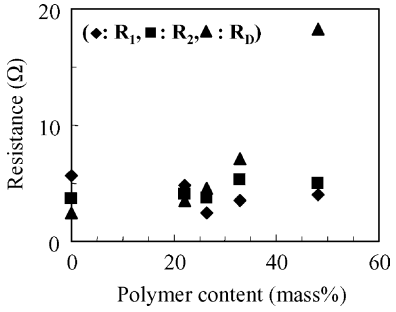

Fig. 5. Polymer content dependence of the resistance of the Pt/PSE interface (R_1), the resistance of the TiO_2/PSE interface (R_2), and the diffusion resistance (R_D).

on; Z_D the finite-length Warburg diffusion impedance; and CPE_i ($i = 1, 2$) the constant phase element. The impedance of the Warburg diffusion in a finite-length region and CPE_i are defined, respectively, by the following equations:

$$Z_D = R_D \left\{ \frac{[\tanh(j\omega\tau)^{1/2}]}{(j\omega\tau)^{1/2}} \right\} \quad (1)$$

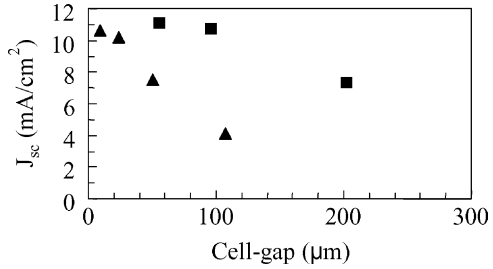

Fig. 6. Dependence of the J_{sc} on the cell gap of liquid electrolyte-based and PSE-based DSSCs: (■) liquid electrolyte-based DSSC; (▲) PSE-based DSSC.

where $\tau = L^2/D_e$, D_e is the effective diffusion coefficient of the diffusing species, and L the effective length:

$$CPE_i = \frac{1}{T_i(j\omega)^P i} \quad (2)$$

where T_i and P_i are parameters obtained by curve fitting. Detailed discussions of these parameters are given elsewhere [24]. The resistances of the Pt/PSE interface (R_1) are plotted in Fig. 5. R_1, unlike the diffusion coefficient, depends hardly on the polymer content. R_1 is the charge transfer resistance at the interface between the PSE film and the Pt counter electrode. Therefore, the decrease in the J_{sc} of the two different kinds of DSSC, given in Fig. 2, results mainly from the decrease in the diffusion coefficient of I_3^-. This fact indicates that the interface between the PSE film and the Pt counter electrode is established in good condition because R_1 would increase in the PSE-based DSSC otherwise.

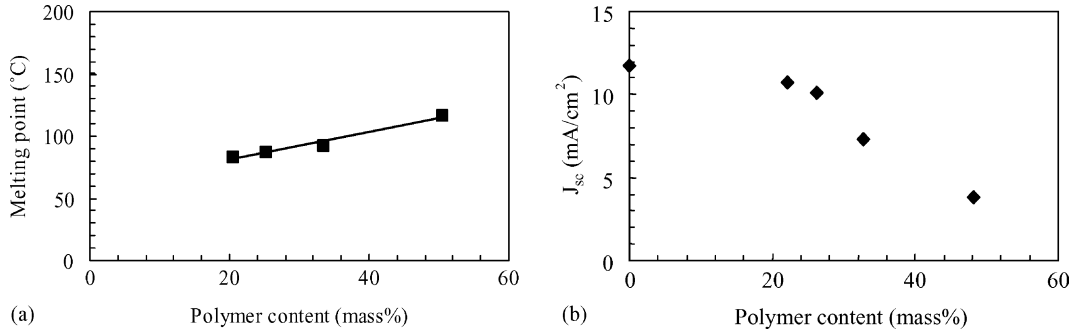

Fig. 7. Melting points of PSE films and the J_{sc} of DSSCs with five different polymer contents.

3.2. The cell-gap dependence of the J_{sc}

Fig. 6 shows the dependence of the J_{sc} on the cell gap of the liquid electrolyte-based and PSE-based DSSCs. The dependence of the J_{sc} becomes weaker in a narrower cell-gap region. The J_{sc} of liquid electrolyte (GBL)-based DSSC is almost constant in cell gaps less than 50 μm, whereas that of the PSE (GBL/matrix polymer = 37.0 mass%)-based DSSC monotonically decreases with the cell gap in the cell-gap region studied. The difference in the cell-gap dependence between the two kinds of DSSCs originates mainly from the difference in the diffusion coefficient. The diffusion coefficient of the PSE is, as given in Table 1, smaller by a factor of about 3.7 than that of the liquid electrolyte.

The melting points of PSE films and the J_{sc} of DSSCs with five different polymer contents are plotted in Fig. 7(a) and (b), respectively. Although the J_{sc} of PSE-based DSSCs increases as the polymer content decreases, the trade-off for decreasing the PVDF-HFP-based polymer content is the diminishment of the PSE tensile strength at high temperatures because the melting point drops. We then employed a PSE film with a 35 mass% polymer content and a 20 μm cell gap, and we confirmed that the J_{sc} of a PSE-based DSSC reached about 97% of that of a liquid electrolyte-based DSSC. The PSE film used in this DSSC was selected to have a melting point of 95 °C, which is high enough for outdoor applications.

4. Conclusion

Electrochemical studies were performed on the two different kinds of DSSCs to explain why the conversion efficiency is lower in PSE-based DSSCs than in liquid electrolyte-based DSSCs. The difference in the J_{sc} between the two different kinds of DSSCs was found out to depend chiefly on the diffusion coefficient of I_3^-. The J_{sc} of the PSE-based DSSC has a strong dependence on the cell gap, and a narrower cell gap gives a higher J_{sc}. The J_{sc} of the PSE-based DSSC with the 20 μm cell gap reaches the value comparable to that of the liquid electrolyte-based DSSC. This fact indicates that the conversion efficiency of the PSE-based DSSC can be improved even higher and equal to that of the liquid electrolyte-based DSSC by optimizing the DSSC structure as well as ingredient of PSE films.

References

[1] H. Tsubomura, M. Matsumura, Y. Nomura, T. Amamiya, Nature 261 (1976) 402.
[2] B. O'Regan, M. Grätzel, Nature 353 (24) (1991) 737.
[3] G. Smestad, C. Bignozzi, R. Argazzi, Sol. Energy Mater. Sol. Cells 32 (1994) 259.
[4] A. Hagfeldt, M. Grätzel, Acc. Chem. Res. 33 (2000) 269.
[5] K. Hara, M. Kurashige, S. Ito, A. Shinpo, S. Suga, K. Sayama, H. Arakawa, Chem. Commun. (2003) 252.
[6] H. Lindström, A. Holmberg, E. Magnusson, S.E. Lindquist, L. Malmqvist, A. Hagfeldt, Nanoletters 1 (2001) 97.
[7] T. Miyasaka, Y. Kijitori, T.N. Murakami, M. Kimura, S. Uegusa, Chem. Lett. (2002) 1250.
[8] P. Wang, S.M. Zakeeruddin, J.E. Moser, M.K. Nazeeruddin, T. Sekiguchi, M. Grätzel, Nat. Mater. 2 (2003) 402.
[9] F. Cao, G. Oskam, C. Searson, J. Phys. Chem. 99 (1995) 17071.
[10] W. Kubo, K. Murakoshi, T. Kitamura, Y. Wada, K. Hanabusa, H. Shirai, S. Yanagida, Chem. Lett. (1998) 1241.
[11] M. Matsumoto, H. Miyazaki, K. Matsuhiro, Y. Kumashiro, Y. Takaoka, Solid State Ionics 89 (1996) 263.
[12] S. Mikoshiba, H. Sumino, M. Yonetsu, S. Hayase, Preprint of 16th European Photovoltaic Solar Energy Conference and Exhibition, Glasgow, 2000.
[13] L. Han, R. Komiya, R. Yamanaka, T. Mitate, Proceedings of the 14th International Conference on Photochemical Conversion and Storage of Solar Energy, W1-O-5, Sapporo, Japan, 2002.
[14] K. Tennakone, G.R.R.A. Kumara, A.R. Kumarasinghe, K.G.U. Wijayantha, P.M. Sirimanne, Semicond. Sci. Technol. 10 (1995) 1689.
[15] K. Tennakone, G.R.R.A. Kumara, I.R.M. Kottegoda, K.G.U. Wijayantha, V.P.S. Perera, J. Phys. D: Appl. Phys. 31 (1998) 1492.
[16] B. O'Regan, D.T. Schwartz, Chem. Mater. 10 (1998) 1501.
[17] B. O'Regan, D.T. Schwartz, S.M. Zakeeruddin, M. Grätzel, Adv. Mater. 12 (2000) 1263.
[18] G. Hagen, D. Haarer, W. Schaffrath, P. Otschik, R. Fink, A. Bacher, H.-W. Schmidt, Synth. Met. 89 (1997) 215.
[19] U. Bach, D. Lupo, P. Comte, J.E. Moser, F. Weissörtel, J. Salbeck, H. Spreitzer, M. Grätzel, Nature 395 (1998) 583.
[20] M. Lorenz, Proceedings of the 12th International Conference on Photochemical Conversion and Storage of Solar Energy, 1W45, Berlin, Germany, 1998.
[21] K. Murakoshi, R. Kogure, Y. Wada, S. Yanagida, Chem. Lett. (1997) 471.
[22] K. Murakoshi, R. Kogure, Y. Wada, S. Yanagida, Sol. Energy Mater. Sol. Cells 55 (1998) 113.
[23] P. Wang, S.M. Zakeeruddin, I. Exnar, M. Grätzel, Chem. Commun. (2002) 2972.
[24] T. Asano, S. Uchida, T. Kubo, Y. Nishikitani, Proceedings of the Third World Conference on Photovoltaic Energy Conversion, 1P-D3-13, Osaka, Japan, 2003.
[25] S. Uchida, M. Kobayashi, T. Kubo, Y. Nishikitani, Proceedings of the 14th International Conference on Photochemical Conversion and Storage of Solar Energy, W1-P-45, Sapporo, Japan, 2002.
[26] A.J. Bard, L.R. Faulkner, Electrochemical Methods: Fundamentals and Applications, 2nd ed., Wiley, New York, 2001, p. 163.
[27] J.O.M. Bockris, A.K.N. Reddy, Modern Electrochemistry, vol. 1, 2nd ed., Plenum Press, New York, 1998, p. 451.
[28] S.Y. Huang, G. Schlichthörl, A.J. Nozik, M. Grätzel, A.J. Frank, J. Phys. Chem. B 101 (1997) 2576.
[29] C. Longo, A.F. Nogueria, M.-A.D. Paoli, J. Phys. Chem. B 106 (2002) 5925.